Hindawi
Complexity
Volume 2019, Article ID 1739785, 13 pages
https://doi.org/10.1155/2019/1739785

*Research Article*

# Numerical Simulation of a Class of Hyperchaotic System Using Barycentric Lagrange Interpolation Collocation Method

**Xiaofei Zhou,[1] Junmei Li,[2] Yulan Wang,[2] and Wei Zhang[1]**

[1] *Institute of Economics and Management, Jining Normal University, Jining 012000, Inner Mongolia, China*
[2] *Department of Mathematics, Inner Mongolia University of Technology, Hohhot 010051, China*

Correspondence should be addressed to Yulan Wang; wylnei@163.com and Wei Zhang; jnsfxyzw@163.com

Received 12 December 2018; Accepted 3 February 2019; Published 13 February 2019

Academic Editor: Diyi Chen



Hyperchaotic system, as an important topic, has become an active research subject in nonlinear science. Over the past two decades, hyperchaotic system between nonlinear systems has been extensively studied. Although many kinds of numerical methods of the system have been announced, simple and efficient methods have always been the direction that scholars strive to pursue. Based on this problem, this paper introduces another novel numerical method to solve a class of hyperchaotic system. Barycentric Lagrange interpolation collocation method is given and illustrated with hyperchaotic system ($\dot{x} = ax + dz - yz, \dot{y} = xz - by,\ \ 0 \le t \le T, \dot{z} = c(x - z) + xy, \dot{w} = c(y - w) + xz,$) as examples. Numerical simulations are used to verify the effectiveness of the present method.

## 1. Introduction

Many chaotic systems have been developed such as Lorenz system [1], Rossler system [2], and Chen system [3]. As chaos theory progresses, many new chaotic systems [4–8] have been proposed, specially hyperchaotic systems [9–15]. A hyperchaotic system is usually characterized as a chaotic system with more than one positive Lyapunov exponent, implying that the dynamics expand in more than one direction, giving rise to more complex chaotic dynamics. Barycentric interpolation collocation method [16, 17] is a high precision method. Some authors have used barycentric interpolation collocation method to solve various kinds of problems [16–23]. This paper suggests the barycentric interpolation collocation method to solve a class of hyperchaotic system, and a hyperchaotic system (1) is adopted as an example to elucidate the solution process.

We consider the following 4D butterfly hyperchaotic system with butterfly phenomenon [24]:

$$\begin{aligned} \dot{x} &= ax + dz - yz, \\ \dot{y} &= xz - by, \quad 0 \le t \le T, \\ \dot{z} &= c(x - z) + xy, \\ \dot{w} &= c(y - w) + xz, \end{aligned} \tag{1}$$

where $x, y, z, w$ are the state variables and $a, b, c, d$ are the positive constant parameters of the system which satisfy the following initial conditions:

$$\begin{aligned} x(0) &= c_1, \\ y(0) &= c_2, \\ z(0) &= c_3, \\ w(0) &= c_4. \end{aligned} \tag{2}$$

## 2. The Numerical Solution of System (1)

First of all, we give initial function $x_0(t), y_0(t)$ and construct the following linear iterative format of system (1):

$$\begin{aligned} \dot{x_n} &= ax_n + dz_n - y_{n-1}z_n, \\ \dot{y_n} &= x_{n-1}z_n - by_n, \quad n = 1, 2, \ldots, \\ \dot{z_n} &= c(x_n - z_n) + x_{n-1}y_n, \\ \dot{w_n} &= c(y_n - w_n) + x_{n-1}z_n, \end{aligned} \tag{3}$$

Next, we use the barycentric Lagrange interpolation collocation method to solve (3).

In the interval $[0,T]$ takes $M$ different nodes, $0 \le t_1 < t_2 < \cdots < t_M \le T$. The barycentric interpolation of $x_n(t), y_n(t), z_n(t), w_n(t) (n = 1,2,3,\cdots)$ can be written as [16, 17]

$$\begin{aligned} x_n(t) &= \sum_{j=1}^{M} \xi_j(t)\, x_n(t_j), \\ y_n(t) &= \sum_{j=1}^{M} \xi_j(t)\, y_n(t_j), \\ z_n(t) &= \sum_{j=1}^{M} \xi_j(t)\, z_n(t_j), \\ w_n(t) &= \sum_{j=1}^{M} \xi_j(t)\, w_n(t_j). \end{aligned} \tag{4}$$

$\xi_j(t) = \omega_j/(t-t_j)/\sum_{k=1}^{M}(\omega_k/(t-t_k))$ is, respectively, barycentric Lagrange interpolation primary function and $\omega_j = 1/\prod_{i=1, j\neq k}^{M}(t_i - t_j)$ is center of gravity interpolation weight.

Use formula (4), the functions $x_n'(t), y_n'(t), z_n'(t), w_n'(t)$ can be expressed as

$$\begin{aligned} x_n'(t) &= \sum_{j=1}^{M} \xi_j'(t)\, x_n(t_j), \\ y_n'(t) &= \sum_{j=1}^{M} \xi_j'(t)\, y_n(t_j), \\ z_n'(t) &= \sum_{j=1}^{M} \xi_j'(t)\, z_n(t_j), \\ w_n'(t) &= \sum_{j=1}^{M} \xi_j'(t)\, w_n(t_j). \end{aligned} \tag{5}$$

So, linear iterative format (3) can be written in following partitioned matrix form:

$$\begin{bmatrix} D - aI & 0 & \operatorname{diag}(y_{n-1}) - dI & 0 \\ 0 & D + bI & -\operatorname{diag}(x_{n-1}) & 0 \\ -cI & \operatorname{diag}(x_{n-1}) & D + cI & 0 \\ 0 & -cI & -\operatorname{diag}(x_{n-1}) & D + cI \end{bmatrix} \begin{bmatrix} x_n \\ y_n \\ z_n \\ w_n \end{bmatrix} = \begin{bmatrix} 0 \\ 0 \\ 0 \\ 0 \end{bmatrix}. \tag{6}$$

The matrix $D = (\xi_j'(t_i))_{i,j=1,2,\cdots M}$ is $M$ order matrix. $I$ is $M$ order unit matrix, diagonal matrix $\operatorname{diag}(x_{n-1}) = \operatorname{diag}(x_{n-1}(t_1), x_{n-1}(t_2), \ldots, x_{n-1}(t_M))$, and diagonal matrix $\operatorname{diag}(y_{n-1}) = \operatorname{diag}(y_{n-1}(t_1), y_{n-1}(t_2), \ldots, y_{n-1}(t_M))$. The vector

Table 1: Parameters used in Experiments 1–5.

| Figures | a | b | c | d | k |
|---|---|---|---|---|---|
| Figure 1 | 1.378 | 0.5 | 0.6 | 0.097 | |
| Figure 2 | 1.378 | 0.5 | 0.6 | 0.097 | |
| Figure 3 | 0.2 | 0.5 | 0.8 | 0.063 | |
| Figure 4 | 0.3 | 0.5 | 0.8 | 0.063 | |
| Figure 5 | 0.6 | 0.5 | 0.8 | 0.063 | |
| Figure 7 | 1 | 0.5 | 2 | 1 | |
| Figure 8 | 1 | 0.5 | 2 | 1 | |
| Figure 9 | 8 | 3 | 4 | -2 | 0.2 |
| Figure 10 | 8 | 3 | 4 | -2 | 0.2 |
| Figure 11 | 15 | 2.5 | 0.75 | 2 | 0.2 |
| Figure 12 | 15 | 2.5 | 0.75 | 2 | 0.2 |

$$\begin{aligned} [x_n, y_n, z_n, w_n] = {} & [x_n(t_1), x_n(t_2), \ldots, x_n(t_M), y_n(t_1), \\ & y_n(t_2), \ldots, y_n(t_M), z_n(t_1), z_n(t_2), \ldots, z_n(t_M), w_n(t_1), \ldots, \\ & w_n(t_M)]. \end{aligned} \tag{7}$$

At last, we use initial conditions (2).

Take formula (4) into initial conditions (2); we can get the following discrete equations of initial conditions:

$$\begin{aligned} \sum_{i=1}^{M} \xi_i(0)\, x_n(t_i) &= c_1, \\ \sum_{i=1}^{M} \xi_i(0)\, y_n(t_i) &= c_2, \\ \sum_{i=1}^{M} \xi_i(0)\, z_n(t_i) &= c_3, \\ \sum_{i=1}^{M} \xi_i(0)\, w_n(t_i) &= c_4. \end{aligned} \tag{8}$$

In this paper, we use displacement method to impose the initial conditions. The detailed procedure is as follows.

The first 1 of (6) are replaced separately by the equation of initial conditions (8) in turn.

So, we can get that $x_n(t_j), y_n(t_j), z_n(t_j), w_n(t_j), (j = 1,2,\cdots M)$ are approximate solution of (1) and (2).

## 3. Numerical Experiment

In this section, six numerical experiments are studied to demonstrate the effectiveness of the present method. All experiments are computed using MatlabR2017a. In Experiments 1–6, we choose Chebyshev nodes, the accuracy of iteration control is $\varepsilon = 10^{-10}$, and the initial iteration value $x_0 = y_0 = z_0 = 0$; $x_1 = y_1 = z_1 = T$. Parameters of the numerical Experiments 1–5 are listed in Table 1.

*Experiment 1.* We consider the following hyperchaotic system [25]:

$$\begin{aligned} \dot{x} &= -y - z - aw, \\ \dot{y} &= x, \end{aligned}$$

$$\dot{z} = b\left(1 - y^2\right) - cz,$$
$$\dot{w} = dx, \tag{9}$$

where $x, y, z, w$ are the state variables and $a, b, c, d$ are the positive parameters of the system, which satisfy the following initial conditions:

$$\begin{aligned} x(0) &= 0, \\ y(0) &= 0, \\ z(0) &= 0, \\ w(0) &= 0.1. \end{aligned} \tag{10}$$

We choose Chebyshev nodes; the number of nodes $M = 40$. Numerical results of Experiment 1 are given in Figures 1 and 2.

Figure 1 is states of the hyperchaotic system for Experiment 1 with $a = 1.378, b = 0.5, c = 0.6, d = 0.097$, which is obtained by using the current method, and $(a)$ is the states of $x$ and $y$ and $(b)$ is the states of $z$ and $w$. Figure 2 is hyperchaotic attractors of the system for Experiment 1 with $a = 1.378, b = 0.5, c = 0.6, d = 0.097$, which is obtained by using the current method. Among them, $(c)$ is the graph projected on $(x, z)$-plane; $(d)$ is the graph projected on $(x, w)$-plane; $(e)$ is the graph projected on $(z, w)$-plane; $(f)$ is the graph in three-dimensional $(x, y, z)$-space.

*Experiment 2.* We consider the following hyperchaotic system [26]:

$$\begin{aligned} \dot{x} &= a\left(y - x\right) + yz, \\ \dot{y} &= cx - y - xz + w, \\ \dot{z} &= xy - bz, \\ \dot{w} &= -xz + dw, \end{aligned} \tag{11}$$

where $x, y, z, w$ are the state variables and $a, b, c, d$ are the positive parameters of the system, which satisfy the following initial conditions:

$$\begin{aligned} x(0) &= 1, \\ y(0) &= 0, \\ z(0) &= 1, \\ w(0) &= 0. \end{aligned} \tag{12}$$

We choose Chebyshev nodes, the number of nodes $M = 40$, and the parameters $b = 0.5, c = 0.8, d = 0.063$. Numerical results of Experiment 2 are given in Figures 3–6.

Figure 3 is phase portraits of a new hyperchaotic system for Experiment 2 with $a = 0.2$ by using the current method. $(a_1)$ is the graph projected on $(x, y)$-plane; $(b_1)$ is the graph projected on $(x, z)$-plane; $(c_1)$ is the graph projected on $(y, z)$-plane; $(d_1)$ is the graph projected on $(y, w)$-plane; $(e_1)$ is the graph projected on $(z, w)$-plane; $(f_1)$ is the three-dimensional $(x, y, z)$ space graph. Figures 4 and 5 are phase portraits of a new hyperchaotic system for Experiment 2 obtained by using the current method with $a = 0.3$ and $a = 0.6$, respectively. Figure 6 is time series plots of a new hyperchaotic system for Experiment 2 with different parameter value $a$. $(a)$ and $(d)$ represent time series when $a = 0.2$; $(b)$ and $(e)$ represent time series when $a = 0.3$; $(c)$ and $(f)$ represent time series when $a = 0.6$.

*Experiment 3.* We consider the following butterfly hyperchaotic system [24]:

$$\begin{aligned} \dot{x} &= ax + dz - yz, \\ \dot{y} &= xz - by, \\ \dot{z} &= c\left(x - z\right) + xy, \\ \dot{w} &= c\left(y - w\right) + xz, \end{aligned} \tag{13}$$

where $x, y, z, w$ are the state variables and $a, b, c, d$ are the positive constant parameters of the system, which satisfy the following initial conditions:

$$\begin{aligned} x(0) &= 1, \\ y(0) &= 0, \\ z(0) &= 1, \\ w(0) &= 0. \end{aligned} \tag{14}$$

We choose Chebyshev nodes; the number of nodes $M = 30$. Numerical results of Experiment 3 are given in Figures 7 and 8.

Figure 7 is states of a novel butterfly hyperchaotic system for Experiment 3 with $a = 1, b = 0.5, c = 2, d = 1$, which is obtained by using the current method, and $(a)$ is the states of $x$ and $y$ and $(b)$ is the states of $z$ and $w$. Figure 8 is phase portraits of a novel butterfly hyperchaotic system for Experiment 3 with $a = 1, b = 0.5, c = 2, d = 1$, which is obtained by using the current method. Among them, $(c)$ is the graph projected on $(x, z)$-plane; $(d)$ is the graph projected on $(x, w)$-plane; $(e)$ is the graph projected on $(y, z)$-plane; $(f)$ is the graph projected on $(z, w)$-plane; $(g)$ is the graph in three-dimensional $(y, z, w)$-space.

*Experiment 4.* We consider the following hyperchaotic Chen system [27]:

$$\begin{aligned} \dot{x} &= a\left(y - x\right), \\ \dot{y} &= \left(d - z\right)x + cy - w, \\ \dot{z} &= xy - bz, \\ \dot{w} &= x + k, \end{aligned} \tag{15}$$

where $x, y, z, w$ are the state variables and $a, b, c, d, k$ are the positive constant parameters of the system, which satisfy the following initial conditions:

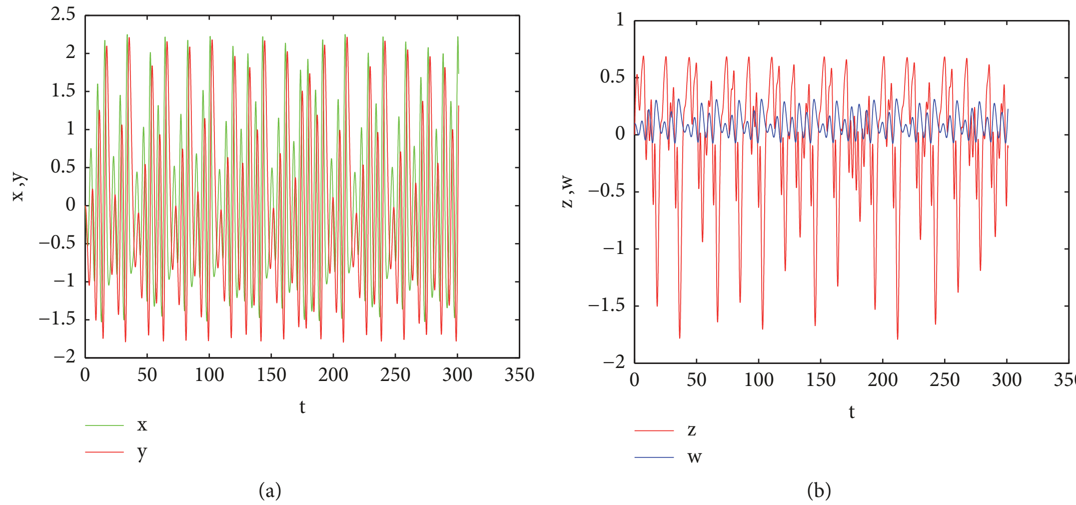


Figure 1: States of the hyperchaotic system for Experiment 1 with $a = 1.378$, $b = 0.5$, $c = 0.6$, and $d = 0.097$: (a) $x$, $y$ states; (b) $z, w$ states.

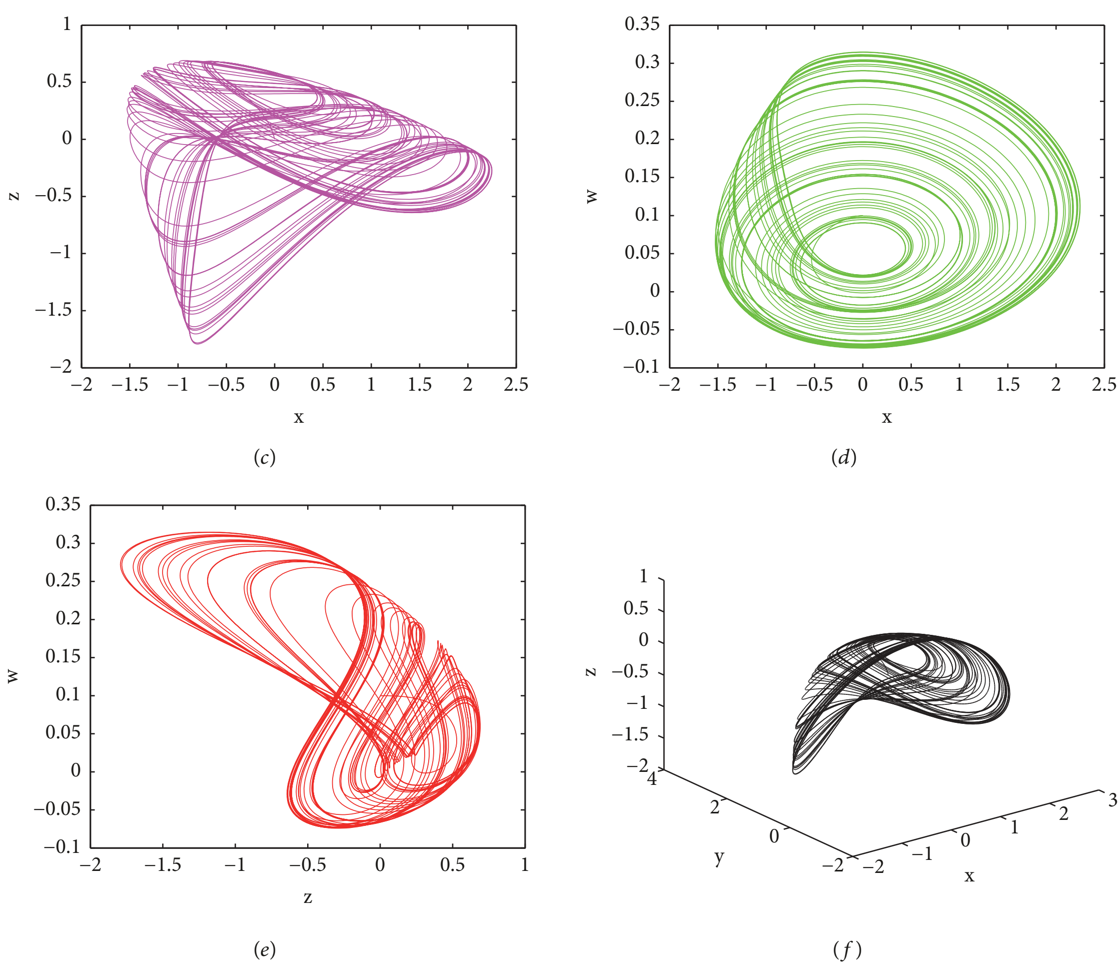


Figure 2: Hyperchaotic attractors of the system for Experiment 1 with $a = 1.378, b = 0.5, c = 0.6, d = 0.097$ (c) on $x - z$ plane, (d) on $x - w$ plane, (e) on $z - w$ plane, and (f) in $x - y - z$ space.

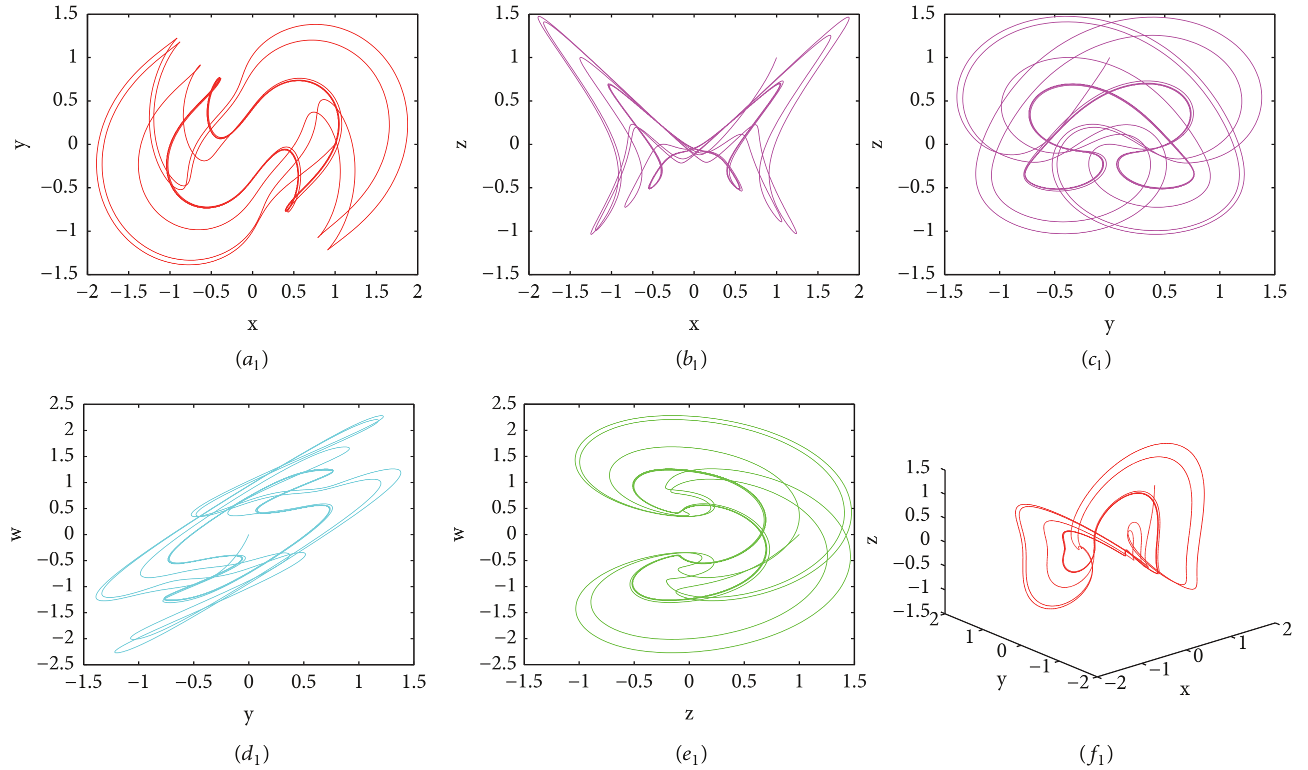


FIGURE 3: Phase portraits of a new hyperchaotic system for Experiment 2 with $a = 0.2$ $(a_1)$ on $x - y$ plane, $(b_1)$ on $x - z$ plane, $(c_1)$ on $y - z$ plane, $(d_1)$ on $y - w$ plane, $(e_1)$ on $z - w$ plane, and $(f_1)$ in $x - y - z$ space.

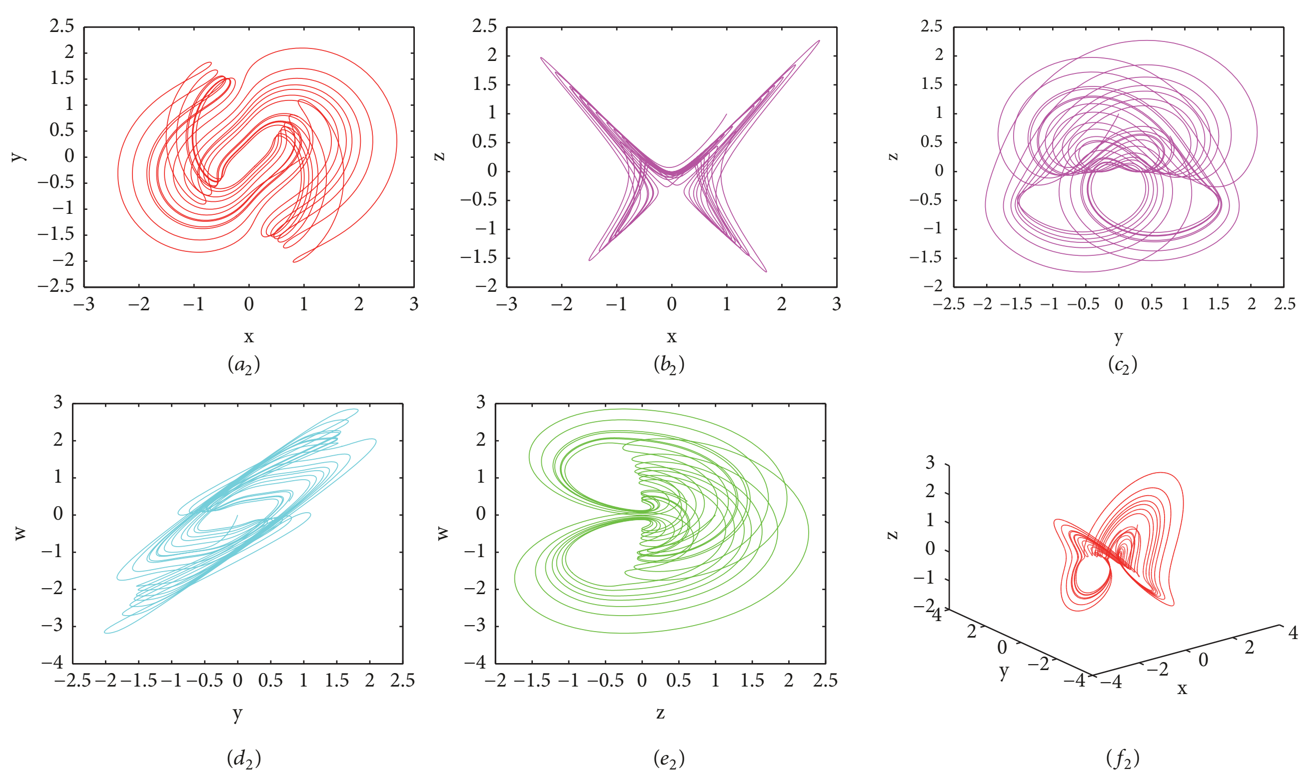


FIGURE 4: Phase portraits of a new hyperchaotic system for Experiment 2 with $a = 0.3$ $(a_2)$ on $x - y$ plane, $(b_2)$ on $x - z$ plane, $(c_2)$ on $y - z$ plane, $(d_2)$ on $y - w$ plane, $(e_2)$ on $z - w$ plane, and $(f_2)$ in $x - y - z$ space.

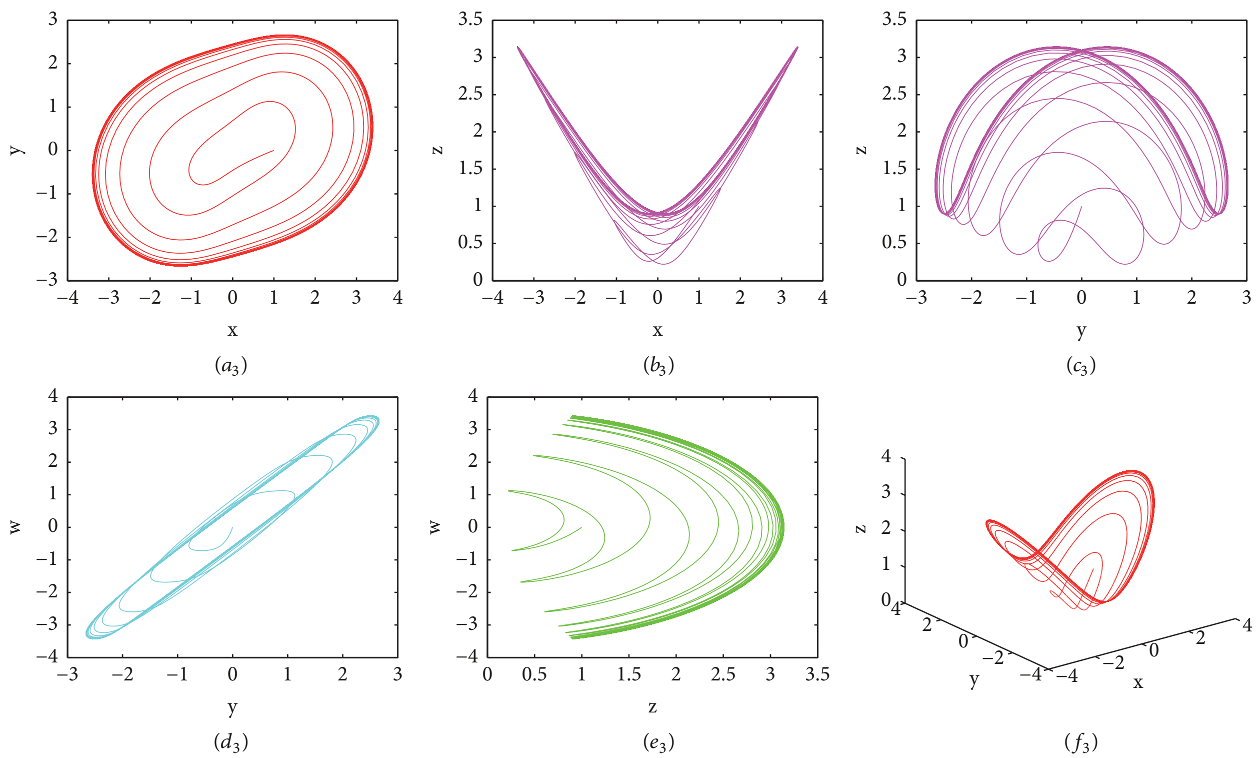


Figure 5: Phase portraits of a new hyperchaotic system for Experiment 2 with $a = 0.6$ $(a_3)$ on $x - y$ plane, $(b_3)$ on $x - z$ plane, $(c_3)$ on $y - z$ plane, $(d_3)$ on $y - w$ plane, $(e_3)$ on $z - w$ plane, and $(f_3)$ in $x - y - z$ space.

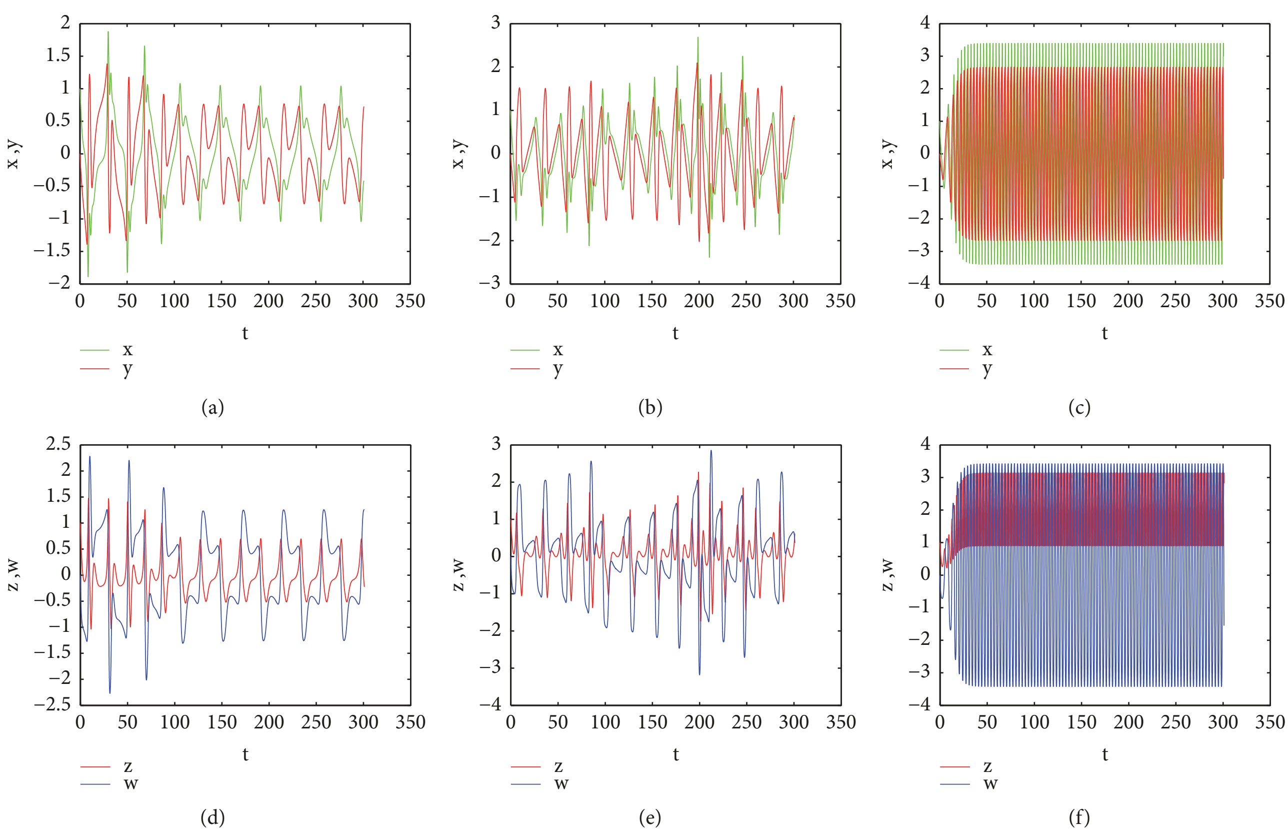


Figure 6: The time series plots of a new hyperchaotic system for Experiment 2. $(a)$ and $(d)$ represent time series when $a = 0.2$; $(b)$ and $(e)$ represent time series when $a = 0.3$; $(c)$ and $(f)$ represent time series when $a = 0.6$.

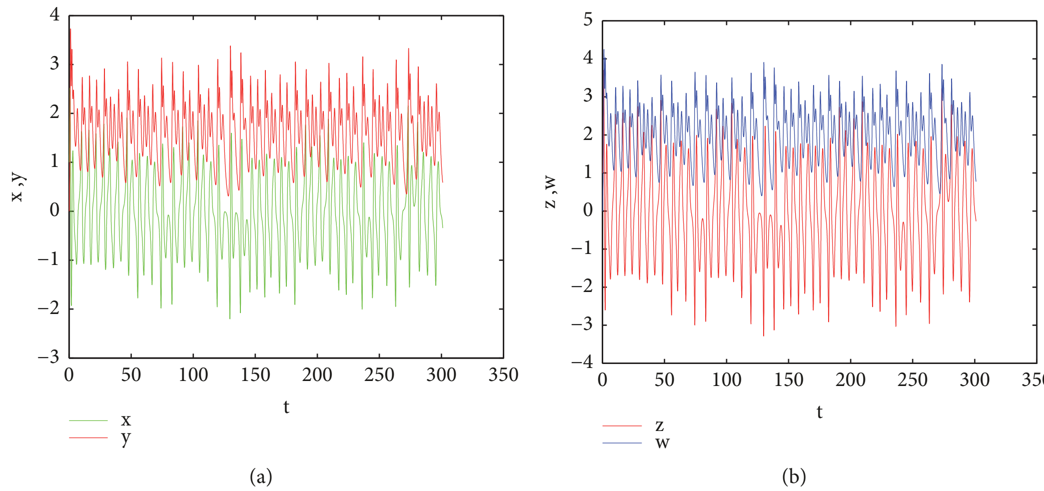


FIGURE 7: States of a novel butterfly hyperchaotic system for Experiment 3 with $a = 1, b = 0.5, c = 2, d = 1$: $(a) x, y$ states; $(b) z, w$ states.

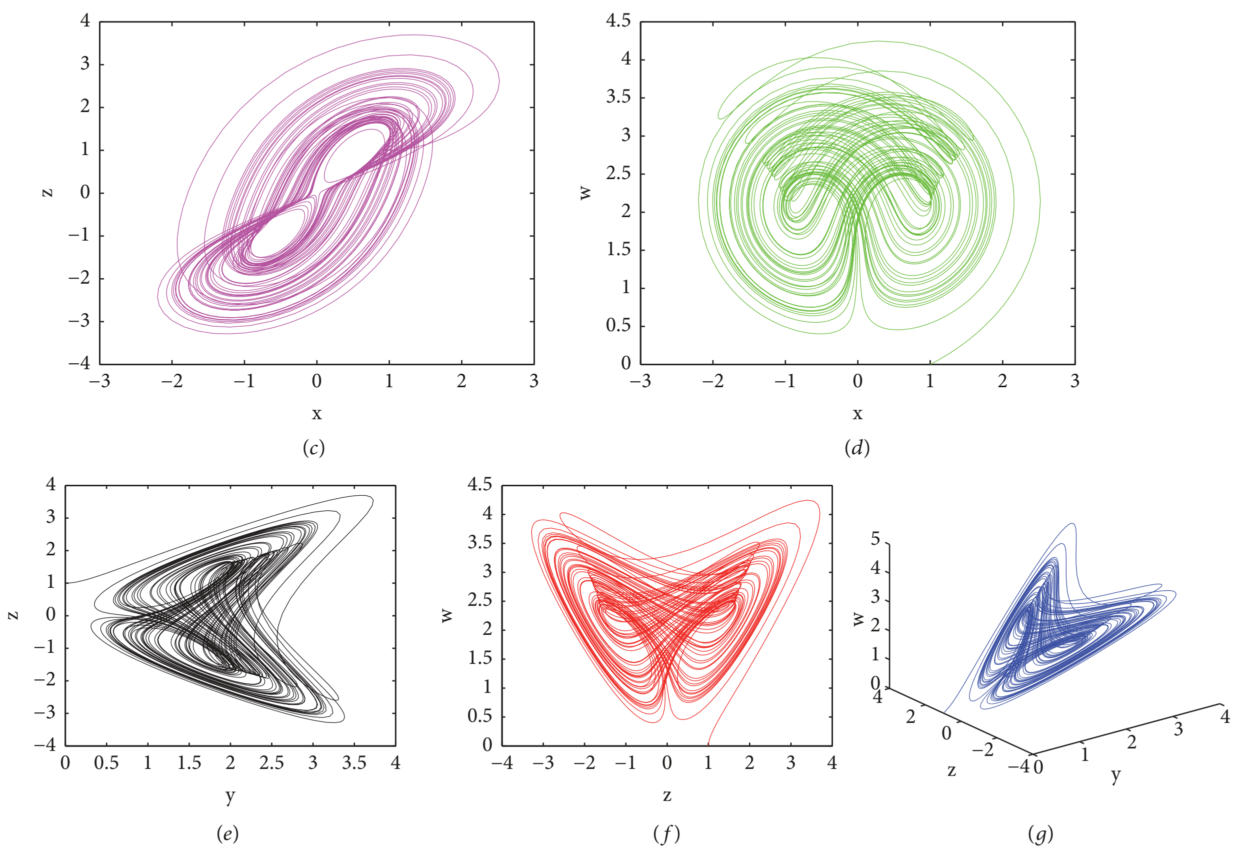


FIGURE 8: Phase portraits of a novel butterfly hyperchaotic system for Experiment 3 with $a = 1, b = 0.5, c = 2, d = 1$ $(c)$ projected on the $(x, z)$-plane, $(d)$ projected on the $(x, w)$-plane, $(e)$ projected on the $(y, z)$-plane, $(f)$ projected on the $(z, w)$-plane, and $(g)$ in the three-dimensional $(y, z, w)$ space.

$$\begin{aligned} x(0) &= 1, \\ y(0) &= 0, \\ z(0) &= 1, \\ w(0) &= 0. \end{aligned} \tag{16}$$

We choose Chebyshev nodes; the number of nodes $M = 35$. Numerical results of Experiment 4 are given in Figures 9 and 10.

Figure 9 is time response of the hyperchaotic Chen system's variable states for Experiment 4 with $a = 8, b = 3, c = 4, d = -2, k = 0.2$, which is obtained by using the current

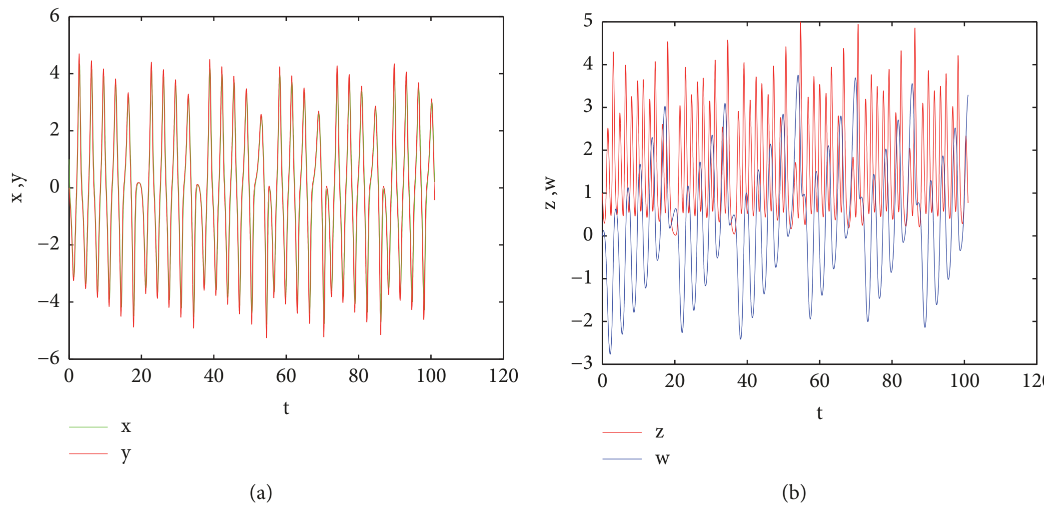


FIGURE 9: Time response of the hyperchaotic Chen system's variable states for Experiment 4 with $a = 8, b = 3, c = 4, d = -2, k = 0.2$: $(a) x, y$ states; $(b) z, w$ states.

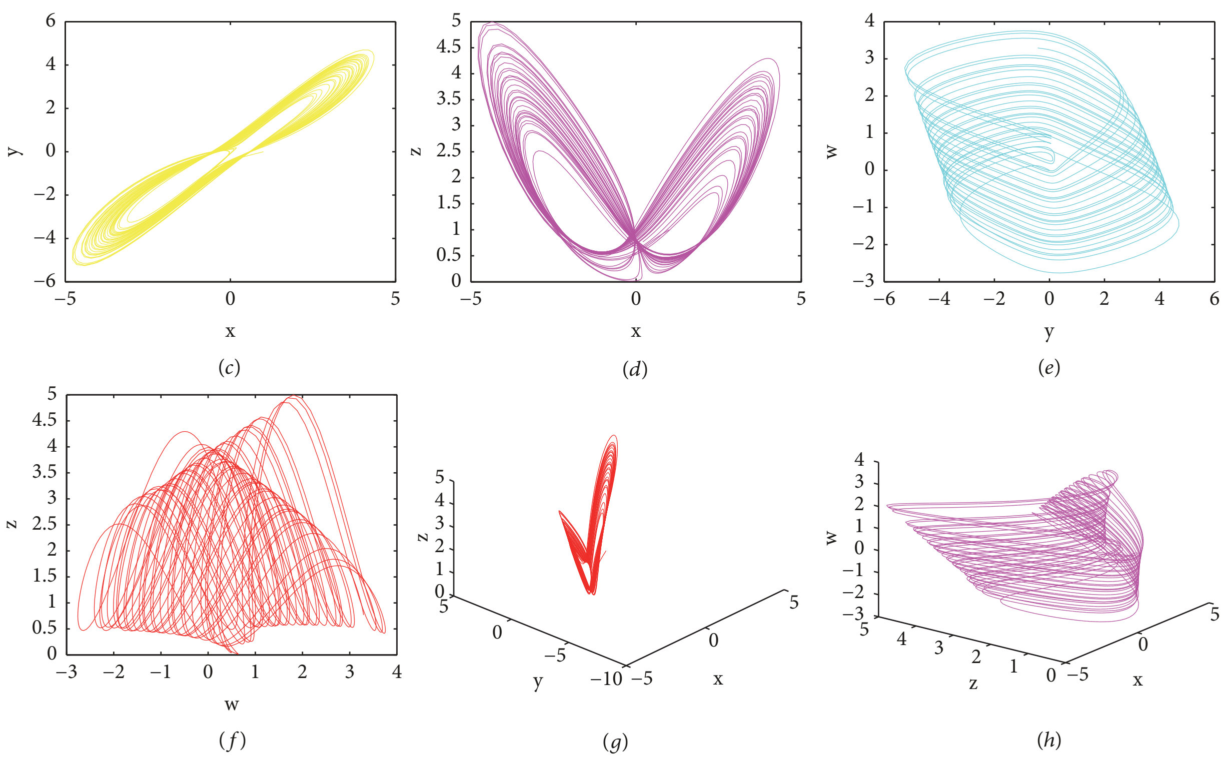


FIGURE 10: The hyperchaotic Chen system for Experiment 4 with $a = 8, b = 3, c = 4, d = -2, k = 0.2$. $(c)$ Phase plane $(x, y)$. $(d)$ Phase plane $(x, z)$. $(e)$ Phase plane $(y, w)$. $(f)$ Phase plane $(w, z)$. $(g)$ in the three-dimensional $(x, y, z)$ space. $(h)$ in the three-dimensional $(x, z, w)$ space.

method, and $(a)$ is the states of $x$ and $y$ and $(b)$ is the states of $z$ and $w$. Figure 10 is phase portraits of the hyperchaotic Chen system for Experiment 4 with $a = 8, b = 3, c = 4, d = -2, k = 0.2$, which is obtained by using the current method. Among them, $(c)$ is the graph projected on $(x, y)$-plane; $(d)$ is the graph projected on $(x, z)$-plane; $(e)$ is the graph projected on $(y, w)$-plane; $(f)$ is the graph projected on $(w, z)$-plane; $(g)$ is the graph in three-dimensional $(x, y, z)$-space; $(h)$ is the graph in three-dimensional $(x, z, w)$-space.

*Experiment 5.* We consider the following hyperchaotic system [28]:

$$
\begin{aligned}
\dot{x} &= a(y - x) + yz, \\
\dot{y} &= cx - xz + kw, \\
\dot{z} &= -bz + xy + 0.5w, \\
\dot{w} &= -dy,
\end{aligned}
\tag{17}
$$

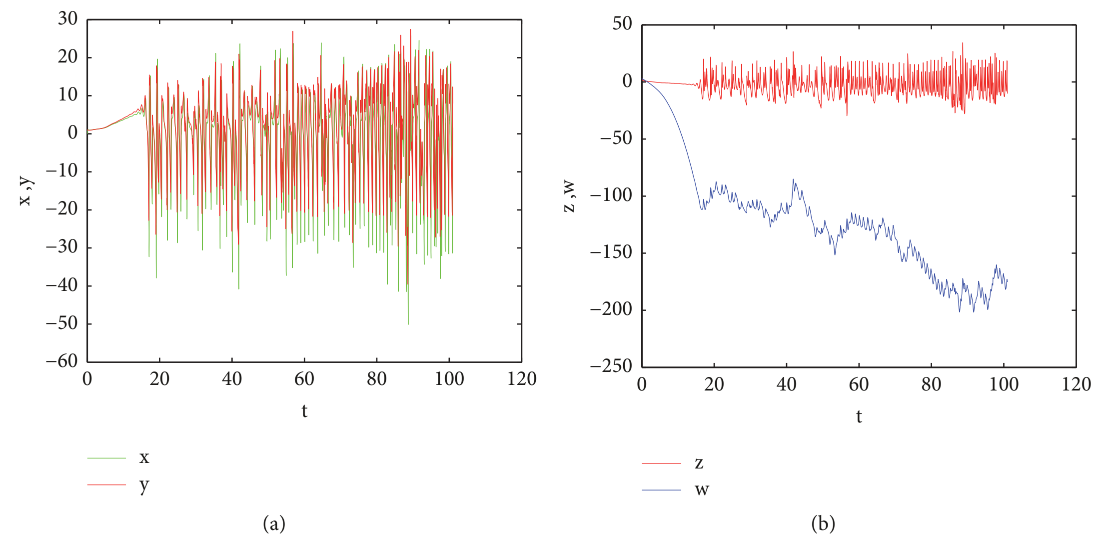


FIGURE 11: The time series plots of a new hyperchaotic system for Experiment 5 with $a = 15, b = 2.5, c = 0.75, d = 2, k = 0.2$: $(a) x, y$ states; $(b) z, w$ states.

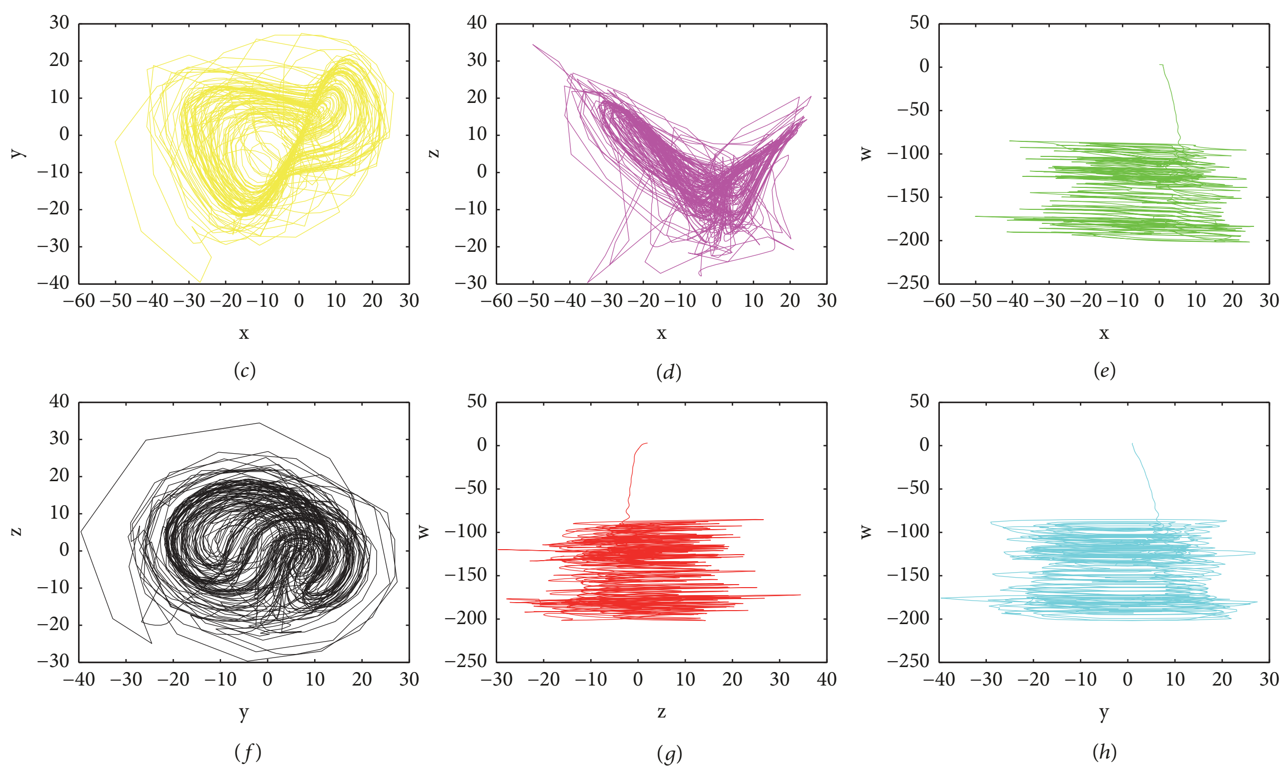


FIGURE 12: Hyperchaotic attractors of a new hyperchaotic system for Experiment 5 with $a = 15, b = 2.5, c = 0.75, d = 2, k = 0.2$. $(c)$ $(x, y)$ plane; $(d)$ $(x, z)$ plane; $(e)$ $(x, w)$ plane; $(f)$ $(y, z)$ plane; $(g)$ $(y, w)$ plane; $(h)$ $(z, w)$ plane.

where $x, y, z, w$ are the state variables and $a, b, c, d, k$ are the positive constant parameters of the system, which satisfy the following initial conditions:

$$
\begin{aligned}
x(0) &= 0, \\
y(0) &= 1, \\
z(0) &= 2, \\
w(0) &= 3.
\end{aligned} \tag{18}
$$

We choose Chebyshev nodes; the number of nodes $M = 40$. Numerical results of Experiment 5 are given in Figures 11 and 12.

Figure 11 is the time series plots of a new hyperchaotic system for Experiment 5 with $a = 15, b = 2.5, c = 0.75, d = 2, k = 0.2$, which is obtained by using the current method, and $(a)$ is the states of $x$ and $y$ and $(b)$ is the states of $z$ and $w$. Figure 12 is hyperchaotic attractors of a new hyperchaotic system for Experiment 5 with $a = 15, b = 2.5, c = 0.75, d = 2, k = 0.2$, which is obtained by using the current method.

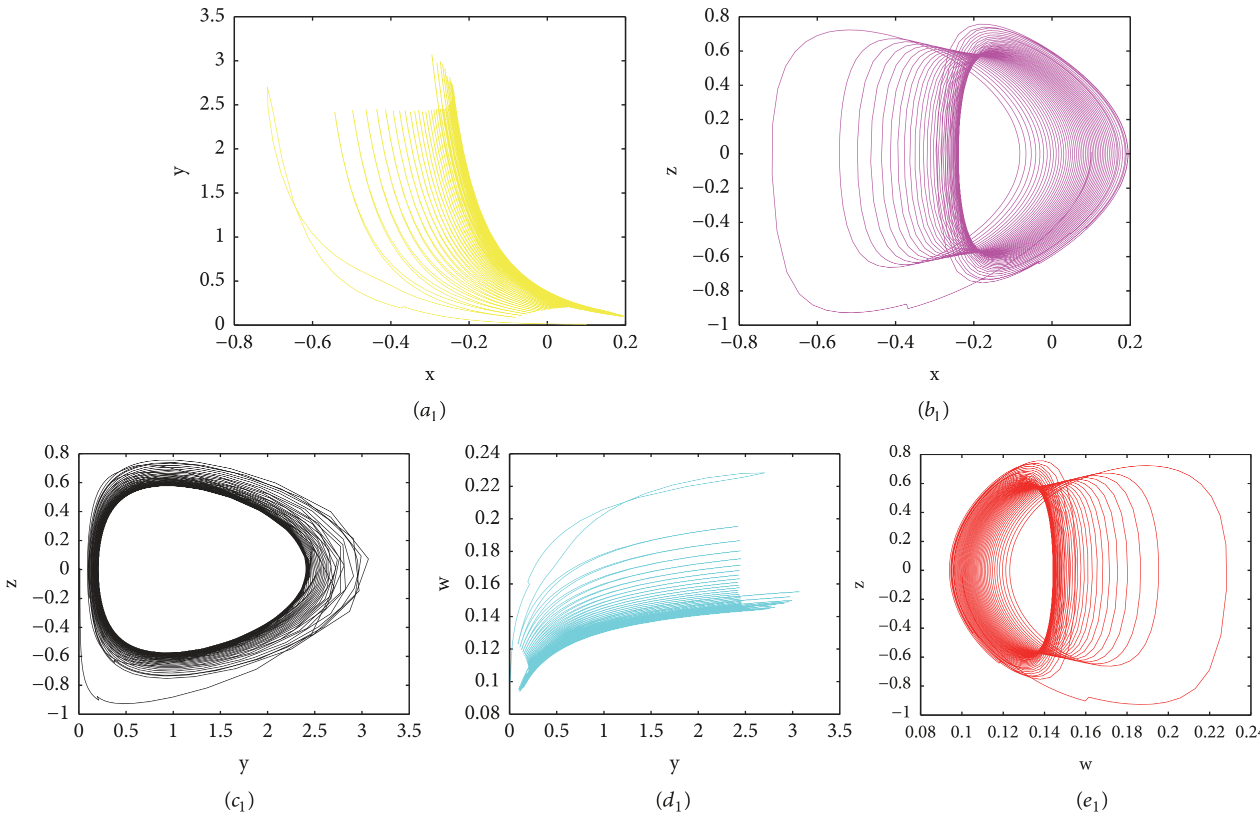


FIGURE 13: Phase portraits of a 4D hyperchaotic system for Experiment 6 with $1/a^2 = 2.7, 1/b^2 = 1, 1/c^2 = 1.5, d = 3, k = 1, h = 5$ $(a_1)$ projected on the $(x, y)$-plane, $(b_1)$ projected on the $(x, z)$-plane, $(c_1)$ projected on the $(y, z)$-plane, $(d_1)$ projected on the $(y, w)$-plane, and $(e_1)$ projected on the $(w, z)$-plane.

Among them, $(c)$ is the graph projected on $(x, y)$-plane; $(d)$ is the graph projected on $(x, z)$-plane; $(e)$ is the graph projected on $(x, w)$-plane; $(f)$ is the graph projected on $(y, z)$-plane; $(g)$ is the graph projected on $(y, w)$-plane; $(h)$ is the graph projected on $(z, w)$-plane.

*Experiment 6.* We consider the following 4D hyperchaotic system [29]:

$$\begin{aligned}
\dot{x} &= z, \\
\dot{y} &= -z\left(hy + dy^2 + xz\right), \\
\dot{z} &= \frac{x^2}{a^2} + \frac{y^2}{b^2} + \frac{w^2}{c^2} - 1, \\
\dot{w} &= -kzw,
\end{aligned} \tag{19}$$

where $x, y, z, w$ are the state variables and $a, b, c, d, k, h$ are the positive constant parameters of the system, which satisfy the following initial conditions:

$$\begin{aligned}
x(0) &= 0.1, \\
y(0) &= 0.01, \\
z(0) &= 0.01, \\
w(0) &= 0.1.
\end{aligned} \tag{20}$$

We choose Chebyshev nodes; the number of nodes $M = 35$. Numerical results of Experiment 6 are given in Figures 13–15.

Figure 13 is phase portraits of a 4D hyperchaotic system for Experiment 6 with $1/a^2 = 2.7, 1/b^2 = 1, 1/c^2 = 1.5, d = 3$, $k = 1$, and $h = 5$, which is obtained by using the current method. Among them, $(a_1)$ is the graph projected on $(x, y)$-plane; $(b_1)$ is the graph projected on $(x, z)$-plane; $(c_1)$ is the graph projected on $(y, z)$-plane; $(d_1)$ is the graph projected on $(y, w)$-plane; $(e_1)$ is the graph projected on $(w, z)$-plane. Figure 14 is phase portraits of a 4D hyperchaotic system for Experiment 6 with $1/a^2 = 3$, $1/b^2 = 3$, $1/c^2 = 3$, $d = 3$, $k = 1$, and $h = 5$, which is obtained by using the current method. Figure 15 is the time series plots of a 4D hyperchaotic system for Experiment 6. $(f_1)$ and $(g_1)$ are obtained by using the current method with $1/a^2 = 2.7$, $1/b^2 = 1$, $1/c^2 = 1.5$, $d = 3$, $k = 1$, and $h = 5$. $(f_2)$ and $(g_2)$ are obtained by using the current method with $1/a^2 = 3$, $1/b^2 = 3$, $1/c^2 = 3$, $d = 3$, $k = 1$, and $h = 5$.

## 4. Conclusions and Remarks

In this paper, a class of hyperchaotic system has been solved by using barycentric Lagrange interpolation collocation method. The numerical simulation results are in accord with the theoretical analyses and circuit implementation.

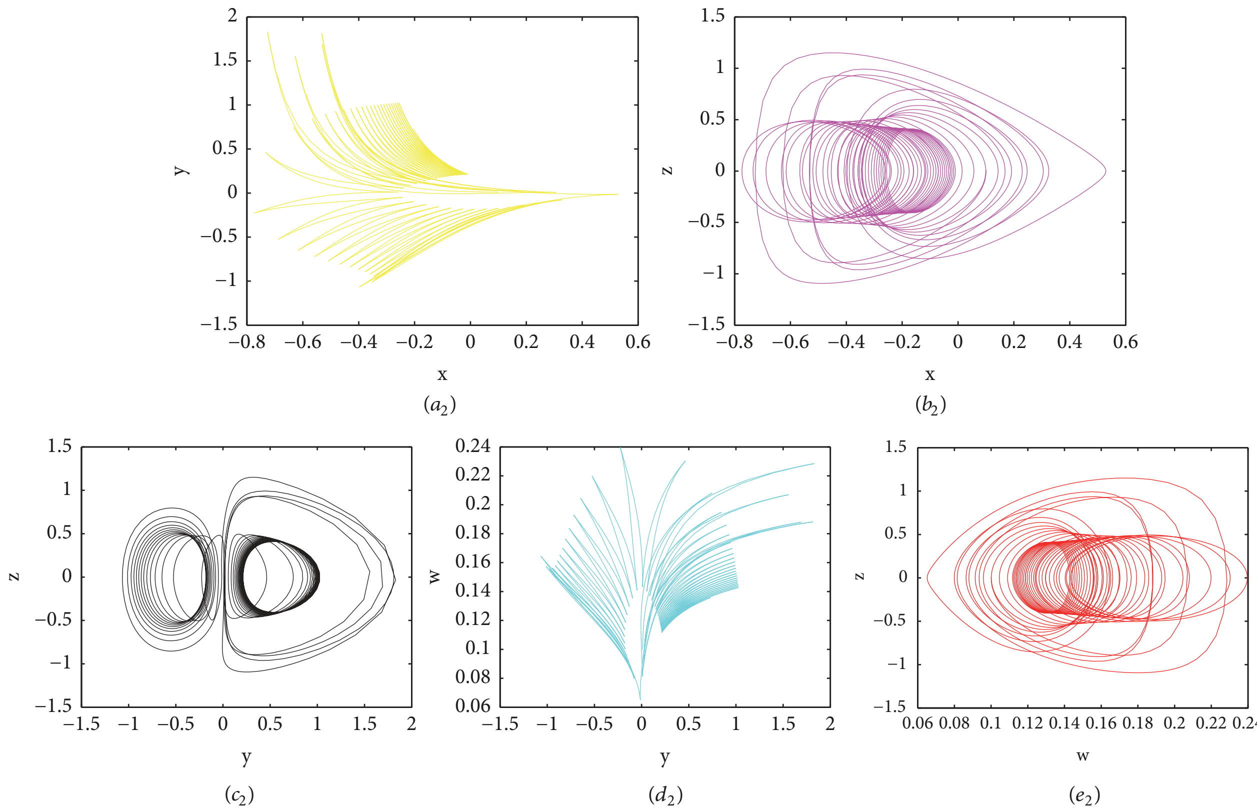


FIGURE 14: Phase portraits of a 4D hyperchaotic system for Experiment 6 with $1/a^2 = 3, 1/b^2 = 3, 1/c^2 = 3, d = 3, k = 1, h = 5$ $(a_2)$ projected on the $(x, y)$-plane, $(b_2)$ projected on the $(x, z)$-plane, $(c_2)$ projected on the $(y, z)$-plane, $(d_2)$ projected on the $(y, w)$-plane, and $(e_2)$ projected on the $(w, z)$-plane.

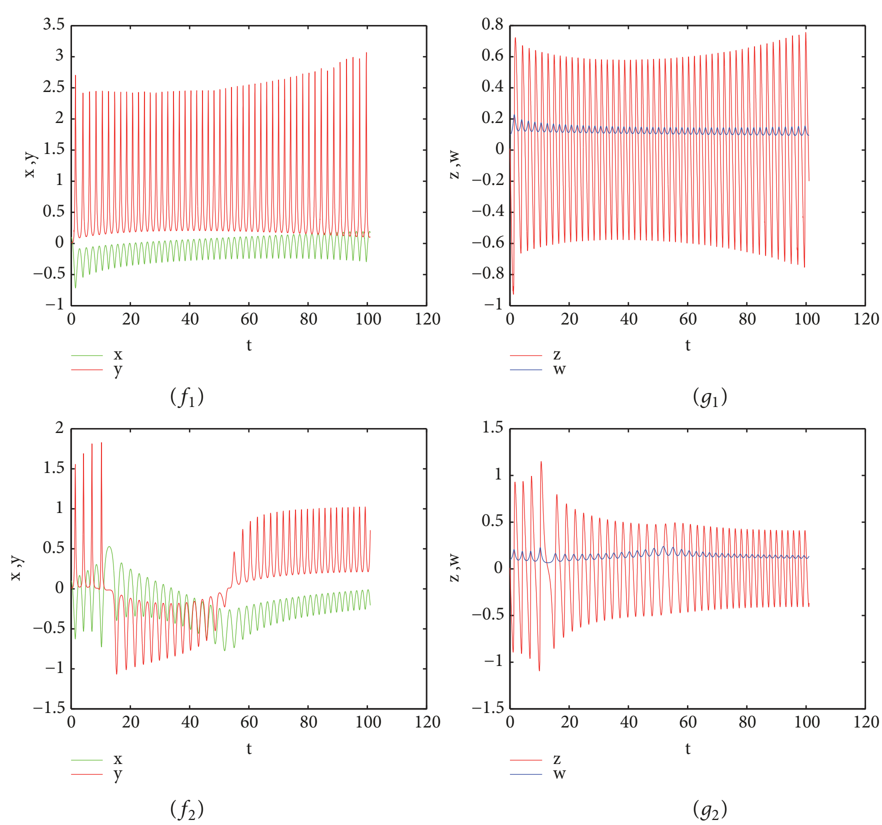


FIGURE 15: The time series plots of a 4D hyperchaotic system for Experiment 6: $(f_1)$ and $(g_1)$ $1/a^2 = 2.7, 1/b^2 = 1, 1/c^2 = 1.5, d = 3, k = 1, h = 5$; $(f_2)$ and $(g_2)$ $1/a^2 = 3, 1/b^2 = 3, 1/c^2 = 3, d = 3, k = 1, h = 5$.

Numerical simulations are provided to verify the effectiveness and feasibility of the proposed numerical results, which are in agreement with theoretical analysis. In the further work, we will be devoted to studying fractional-order hyperchaotic system.

## Data Availability

The data used to support the findings of this study are available from the corresponding author upon request.

## Conflicts of Interest

The authors declare that there are no conflicts of interest regarding the publication of this article.

## Acknowledgments

This paper is supported by the Natural Science Foundation of Inner Mongolia [2017MS0103], Inner Mongolia maker Collaborative Innovation Center of Jining Normal University, and the National Natural Science Foundation of China [11361037].

## References

[1] E. N. Lorenz, "Deterministic non-periodic flow," *Journal of the Atmospheric Sciences*, vol. 20, pp. 130–141, 1963.

[2] O. E. Rössler, "An equation for continuous chaos," *Physics Letters A*, vol. 57, no. 5, pp. 397-398, 1976.

[3] G. Chen and T. Ueta, "Yet another chaotic attractor," *International Journal of Bifurcation and Chaos*, vol. 9, no. 7, pp. 1465-1466, 1999.

[4] D. Chen, R. Zhang, J. C. Sprott, H. Chen, and X. Ma, "Synchronization between integer-order chaotic systems and a class of fractional-order chaotic systems via sliding mode control," *Chaos: An Interdisciplinary Journal of Nonlinear Science*, vol. 22, no. 2, Article ID 023130, 2012.

[5] A. E. Matouk, A. A. Elsadany, E. Ahmed, and H. N. Agiza, "Dynamical behavior of fractional-order Hastings-Powell food chain model and its discretization," *Communications in Nonlinear Science and Numerical Simulation*, vol. 27, no. 1–3, pp. 153–167, 2015.

[6] D. Y. Chen, R. F. Zhang, J. C. Sprott, and X. Y. Ma, "Synchronization between integer-order chaotic systems and a class of fractional-order chaotic system based on fuzzy sliding mode control," *Nonlinear Dynamics*, vol. 70, no. 2, pp. 1549–1561, 2012.

[7] D. Y. Chen, W. L. Zhao, J. C. Sprott, and X. Ma, "Application of Takagi-Sugeno fuzzy model to a class of chaotic synchronization and anti-synchronization," *Nonlinear Dynamics*, vol. 73, no. 3, pp. 1495–1505, 2013.

[8] D. Y. Chen, C. Wu, H. H. C. Iu, and X. Ma, "Circuit simulation for synchronization of a fractional-order and integer-order chaotic system," *Nonlinear Dynamics*, vol. 73, no. 3, pp. 1671–1686, 2013.

[9] Z. Chen, Y. Yang, G. Qi, and Z. Yuan, "A novel hyperchaos system only with one equilibrium," *Physics Letters A*, vol. 360, no. 6, pp. 696–701, 2007.

[10] X. Wang and M. Wang, "A hyperchaos generated from Lorenz system," *Physica A: Statistical Mechanics and Its Applications*, vol. 387, no. 14, pp. 3751–3758, 2008.

[11] A. E. Matouk, "Dynamics and control in a novel hyperchaotic system," *International Journal of Dynamics and Control*, 2018.

[12] N. Yujun, W. Xingyuan, W. Mingjun, and Z. Huaguang, "A new hyperchaotic system and its circuit implementation," *Communications in Nonlinear Science and Numerical Simulation*, vol. 15, no. 11, pp. 3518–3524, 2010.

[13] A. M. A. El-Sayed, H. M. Nour, A. Elsaid, A. E. Matouk, and A. Elsonbaty, "Circuit realization, bifurcations, chaos and hyperchaos in a new 4D system," *Applied Mathematics and Computation*, vol. 239, pp. 333–345, 2014.

[14] S. Pang and Y. Liu, "A new hyperchaotic system from the Lü system and its control," *Journal of Computational and Applied Mathematics*, vol. 235, no. 8, pp. 2775–2789, 2011.

[15] X. Liu, X. Shen, and H. Zhang, "Multi-scroll chaotic and hyperchaotic attractors generated from Chen system," *International Journal of Bifurcation and Chaos*, vol. 22, Article ID 1250033, 2012.

[16] S. P. Li and Z. Q. Wang, *Barycentric Interpolation Collocation Method for Nonlinear Problems*, National Defense Industry Press, Beijing, China, 2015.

[17] S. P. Li and Z. Q. Wang, *High-Precision Non-Grid Center of Gravity Interpolation Collocation Method: Algorithm, Program And Engineering Application*, Science Press, Beijing, China, 2012.

[18] H. Liu, J. Huang, Y. Pan, and J. Zhang, "Barycentric interpolation collocation methods for solving linear and nonlinear high-dimensional Fredholm integral equations," *Journal of Computational and Applied Mathematics*, vol. 327, pp. 141–154, 2018 (Basque).

[19] W.-H. Luo, T.-Z. Huang, X.-M. Gu, and Y. Liu, "Barycentric rational collocation methods for a class of nonlinear parabolic partial differential equations," *Applied Mathematics Letters*, vol. 68, pp. 13–19, 2017.

[20] F. F. Liu, Y. L. Wang, and S. G. Li, "Barycentric interpolation collocation method for solving the coupled viscous Burgers' equations," *International Journal of Computer Mathematics*, vol. 95, pp. 2162–2173, 2018.

[21] Y. L. Wang, D. Tian, and Z. Y. Li, "Numerical method for singularly perturbed delay parabolic partial differential equations," *Thermal Science*, vol. 21, no. 4, pp. 1595–1599, 2017.

[22] S. P. Li and Z. Q. Wang, "Barycentric interpolation collocation method for solving elastic problems," *Zhongnan Daxue Xuebao (Ziran Kexue Ban)/Journal of Central South University (Science and Technology)*, vol. 44, pp. 2031–2040, 2013.

[23] S. P. Li and Z. Q. Wang, "Barycentric interpolation collocation method for solving nonlinear vibration problems," *Noise Vibration Control*, vol. 28, pp. 49–52, 2018.

[24] L. Zhang, "A novel 4-D butterfly hyperchaotic system," *Optik - International Journal for Light and Electron Optics*, vol. 131, pp. 215–220, 2017.

[25] J. P. Singh and B. K. Roy, "A novel hyperchaotic system with stable and unstable line of equilibria and sigma shaped Poincare map," *IFAC-PapersOnLine*, vol. 49, no. 1, pp. 526–531, 2016.

[26] A. E. Matouk, "On the periodic orbits bifurcating from a fold Hopf bifurcation in two hyperchaotic systems," *Optik - International Journal for Light and Electron Optics*, vol. 126, no. 24, pp. 4890–4895, 2015.

[27] D. Sadaoui, A. Boukabou, and S. Hadef, "Predictive feedback control and synchronization of hyperchaotic systems," *Applied Mathematics and Computation*, vol. 247, pp. 235–243, 2014.

[28] C.-L. Li, J.-B. Xiong, and W. Li, "A new hyperchaotic system and its generalized synchronization," *Optik-International Journal for Light and Electron Optics*, vol. 125, no. 1, pp. 575–579, 2014.

[29] J. P. Singh, B. K. Roy, and S. Jafari, "New family of 4-D hyperchaotic and chaotic systems with quadric surfaces of equilibria," *Chaos, Solitons & Fractals*, vol. 106, pp. 243–257, 2018.


Advances in Operations Research
Advances in Decision Sciences
Journal of Applied Mathematics
The Scientific World Journal
Journal of Probability and Statistics
International Journal of Mathematics and Mathematical Sciences
Hindawi
Submit your manuscripts at
www.hindawi.com
Journal of Optimization
International Journal of Engineering Mathematics
International Journal of Analysis
Journal of Complex Analysis
Advances in Numerical Analysis
Mathematical Problems in Engineering
International Journal of Differential Equations
Discrete Dynamics in Nature and Society
International Journal of Stochastic Analysis
Journal of Mathematics
Journal of Function Spaces
Abstract and Applied Analysis
Advances in Mathematical Physics